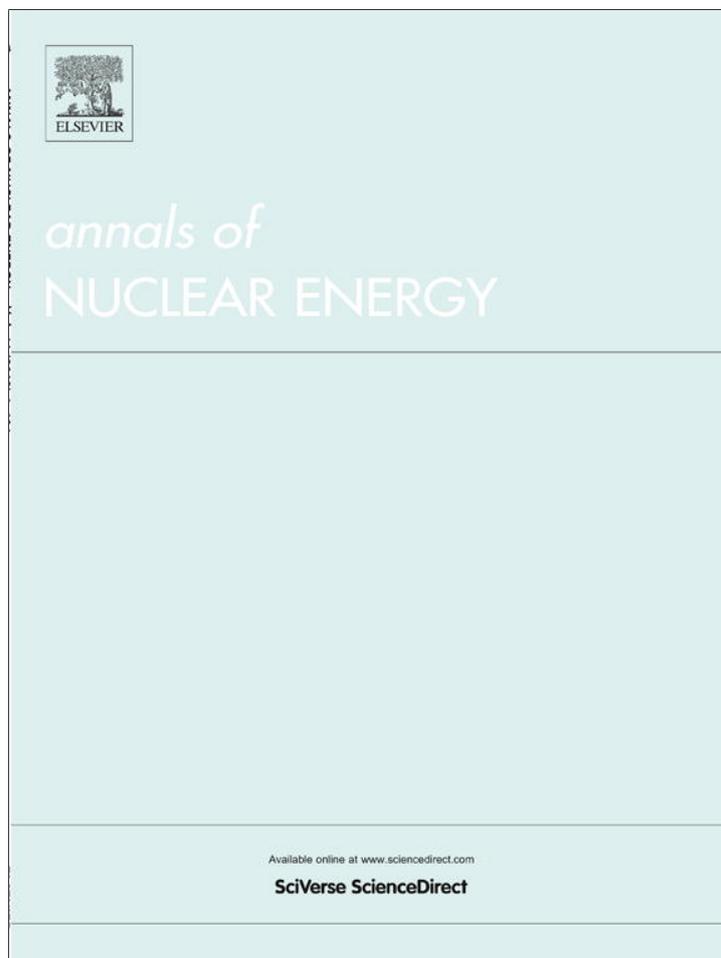


Provided for non-commercial research and education use.
Not for reproduction, distribution or commercial use.



(This is a sample cover image for this issue. The actual cover is not yet available at this time.)

This article appeared in a journal published by Elsevier. The attached copy is furnished to the author for internal non-commercial research and education use, including for instruction at the authors institution and sharing with colleagues.

Other uses, including reproduction and distribution, or selling or licensing copies, or posting to personal, institutional or third party websites are prohibited.

In most cases authors are permitted to post their version of the article (e.g. in Word or Tex form) to their personal website or institutional repository. Authors requiring further information regarding Elsevier's archiving and manuscript policies are encouraged to visit:

<http://www.elsevier.com/copyright>

Contents lists available at [SciVerse ScienceDirect](http://www.sciencedirect.com)

Annals of Nuclear Energy

journal homepage: www.elsevier.com/locate/anucene

Comparison of shielding properties for ordinary, barite, serpentine and steel–magnetite concretes using MCNP-4C code and available experimental results

Sh. Sharifi^a, R. Bagheri^b, S.P. Shirmardi^{c,*}^a Department of Civil Engineering, Islamic Azad University, Maku Branch, Maku, Iran^b Faculty of Nuclear Engineering and Physics, Amirkabir University of Technology, Tehran, Iran^c Nuclear Fuel Cycle Research School (NFCRS), Nuclear Science and Technology Research Institute (NSTRI), Tehran 14155-1339, Iran

ARTICLE INFO

Article history:

Received 16 May 2012

Received in revised form 2 September 2012

Accepted 8 September 2012

Keywords:

Concrete

Shielding

MCNP-4C

Gamma-ray

Linear attenuation coefficients

ABSTRACT

In this paper shielding properties of ordinary, barite, serpentine and steel–magnetite concretes in 511, 662 and 1332 keV gamma ray energies were studied using MCNP-4C code and compared with available experimental results. The simulated and measured values were compared and the results showed reasonable agreement for all concretes. Steel–magnetite has higher linear and mass attenuation coefficients, and lower transmission factor, HVL and TVL values relative to other concretes in each photon energies studied in this research.

© 2012 Elsevier Ltd. All rights reserved.

1. Introduction

Application and development of nuclear science and technology in different fields such as cancer treatment centers, nuclear power plants, nuclear research reactors, collegiate test reactors, national laboratories and research facilities has set human beings in serious exposures from ionization radiations, therefore provision of reasonable and adequate shielding in these places remains an important obligation in establishment of nuclear facilities (Eakins, 2007; Akkurt et al., 2010). Radiation safety practice is a special aspect of the control of environmental health hazards by engineering means, so population and workers exposure from ionization radiations in working and public areas must be kept under the maximum permissible dose suggested by ICRP basic radiation safety criteria (Cember and Johnson, 2009).

Usually ordinary and heavy weight concretes are used for radiation shielding, for both medical and nuclear purposes to prevent population and employment staff exposure versus ionization radiation. Depend on several factors such as cost and abundance of shielding materials, energy and type of radiation, various type concretes with and without dense mineral aggregates are utilized in protective shielding concretes against ionization radiations (Bouzarjomehri et al., 2006).

Depending on the type of aggregate with various elemental and structural compositions, various heavy density concretes will obtain. By using of barite and magnetite ores the density of concretes will be over 3500 kg/m³, which is much greater than that of ordinary concrete. Application of serpentine minerals with plenty of hydrogenous materials as aggregate in shielding concrete will result about 2600 kg/m³ in density which is close to ordinary concrete density that spans from 2200 to 2500 kg/m³. This type of aggregate mostly is used for neutron shielding (Bashter, 1997).

Water/cement ratios in high density concretes are similar to those for ordinary concretes (approximately half time), but the aggregate/cement ratios will be significantly higher, because of the higher density of the aggregates. Percentage composition of four types of concrete studied at this research and their densities are given in Table 1.

The radiation shielding properties of materials are expressed with the term of linear attenuation coefficients. The linear attenuation coefficient (μ) is defined as the fractional decrease, or attenuation of the gamma-ray beam intensity in good geometry per unit thickness of absorber, as defined by the following equation:

$$\lim_{\Delta t \rightarrow 0} \frac{\Delta I}{I \Delta t} = -\mu \quad (1)$$

where $\Delta I/I$ is the fraction of the gamma-ray beam attenuated by an absorber of thickness Δt (Cember and Johnson, 2009). In other words linear attenuation coefficient is defined as the probability of radiation interacting with a material per unit path length.

* Corresponding author. Tel./fax: +98 9126864850.

E-mail address: p_shirmardi@aut.ac.ir (S.P. Shirmardi).

Table 1
Percentage composition for four types of concrete and their densities.

Raw material	Concrete type			
	Ordinary	Barite	Serpentine	Steel-magnetite
Portland cement	11.82	10.77	15.94	7.55
Sand	26.71	–	27.35	–
Gravel	54.96	–	–	–
Barite	–	83.75	–	–
Serpentine	–	–	48.33	–
Magnetite	–	–	–	26.19
Steel scrap	–	–	–	61.73
Water	6.51	5.48	8.38	4.53
Density (g cm ⁻³)	2.3	3.35	2.6	5.1

In this article we studied three important gamma ray energies, 511 keV (annihilation phenomenon), 662 keV (Cs-137) and 1332 keV (Co-60). The gamma irradiations with 511 keV energies are produced from annihilation of positrons emitted from positron-emitter radioisotopes which are used in positron emission tomography (PET) scanning, for example, during the handling and working with positron emitters such as ¹⁸F and ¹³N (Stankovic et al., 2010). Cesium-137(Cs-137) which is a radioactive isotope of cesium formed as a fission product by nuclear fission and emitter of about 662 keV gamma ray energy, in small amounts are used to calibrate radiation-detection equipment and as a gamma emitter for oilfield wireline density measurements. It is also sometimes used in cancer treatment, for sterilization activities for food products and medical equipment and it is also used industrially in gauges for measuring liquid flows and the thickness of materials (<http://www.epa.gov>).

In the last, Cobalt-60 (Co-60) is a neutron activation product radioisotope and emits two gamma rays, 1173 and 1332 keV that are highly penetrating. Due to its half-life of 5.27 years, main uses for Co-60 are: as a tracer for cobalt in chemical reactions, sterilization of medical equipment, radiation source for medical radiotherapy, radiation source for industrial radiography, radioactive source for leveling devices and thickness gauges, as a radioactive source for food irradiation and blood irradiation, and as a radioactive source for laboratory use (<http://www.gammarad.it>). Mentioned numerous applications of these three gamma ray source justify necessity of designing and research on the shielding properties of several concrete used against these radiations in nuclear and medical centers.

In order to compare, verification and validation of experimental results of shielding properties of several concretes mentioned above and validity evaluation of MCNP code usage for simulation of desired concretes prior to experimental and constructional works, this code was considered in this research. MCNP code is a general-purpose Monte Carlo radiation transport code for modeling the interaction of radiation with matter. It utilizes the nuclear cross section libraries and uses physics models for particle interactions and gives required quantity with certain error (Shultis and Faw, 2010).

2. Materials and methods

2.1. Geometry of modeled concrete samples

Cylindrical geometries were employed for modeling of concrete samples corresponding to geometry used in article of Stankovic et al. (2010). In the study of every type of concrete, a series of sub-cylinders with 100 cm in diameter and 10 cm in thickness were considered and set on Z axis in tandem.

2.2. Source specification

Sources were specified as planar, collimated beam and monoenergetic source energies with uniform distribution of radioactive

material (Cs-137,Co-60 and hypothetically 511 keV gamma ray sources) upon them that emit gamma rays perpendicular to front face of shields and parallel in direction of sub-cylinders same axis (in direction of Z axis). These hypothetical source energies were assumed as a disc with 100 cm diameter (no real sizes) and parallel to X–Y plane and origin on Z axis in input script of MCNP code. Such source definition and problem geometry is exactly identical with simulation by FOTLEP-2K6 Monte Carlo code.

2.3. Materials specification of concretes

For comparison of MCNP-4C calculations with data provided in documents, it is tried to specify atomic composition of any concrete types to be same elemental composition reported in articles. The elemental composition of concrete depends mainly on the mix proportions and the chemical composition of the materials used. The percentages by weight of the different elements in the four mentioned shield concretes are presented in Table 2.

2.4. Tally definition

Tally F6 was used to obtain MCNP-4C simulation data. This tally calculates energy deposition in any cell (dosimetric volume) for only one gamma photon that enters the cell and deposits its energy in that cell. Output is represented in MeV/g that g denotes the mass of material enclosed in cell. In this research regarding to geometry approximations considered in Stankovic et al. (2010), a small cylinder of air with 2 cm in diameter and 0.1 cm in thickness were considered as dosimetric volume and set behind sub-cylinders in the 50 cm far from origin on Z axis. Air density (12.0510⁻⁴ g cm⁻³) is chemically specified in accordance with the recommendations of ICRU Report 37 (Brice and David, 1984). Fig. 1 shows modeled concrete samples, collimated beam source energy, source position and dosimetric volume in this simulated geometry.

Depending on thickness of concrete specimens, simulations were performed with 100 million to 2 billion histories. All simulation data obtained by MCNP-4C code were reported with less than 3% error.

3. Results

3.1. Transmission factor

The transmission factors of any type of concrete, $T(E, d)$, for gamma of energy E through thickness d (cm) of shielding concrete

Table 2
The percentage of atomic composition for four types of concrete.

Element	Atomic number	Concrete type			
		Ordinary	Barite	Serpentine	Steel-magnetite
Hydrogen	1	2.21	0.36	7.20	0.51
Carbon	6	0.25	–	0.15	–
Oxygen	8	57.75	31.18	55.6	15.7
Sodium	11	1.52	–	–	–
Magnesium	12	0.13	0.11	10.20	0.58
Aluminum	13	2.10	0.42	2.50	0.66
Silicon	14	30.56	1.04	17.55	2.68
Phosphorus	15	–	–	–	0.08
Sulphur	16	–	10.78	–	0.06
Potassium	19	1.08	–	0.08	–
Calcium	20	4.39	5.02	5.64	3.95
Manganese	25	–	–	–	0.07
Iron	26	0.70	4.75	1.08	75.73
Barium	56	–	46.34	–	–

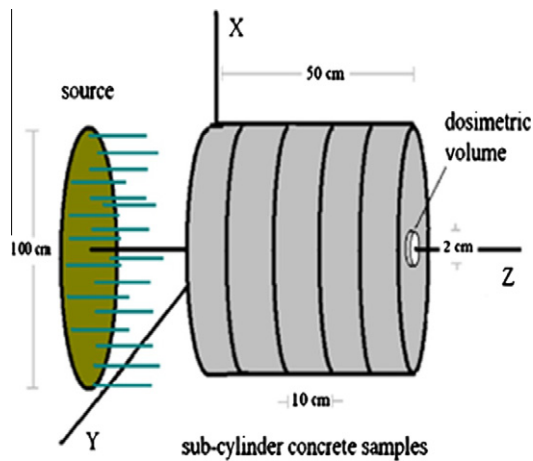


Fig. 1. Geometry of modeled configuration.

was defined by dividing absorbed dose value, $D(E, d)$, attained by the Tally F6 in the dosimetric volume located behind thickness d (cm) of shielding sub-cylinders in the 50 cm far from origin on Z axis to the absorbed dose value, $D(E, 0)$, in the same dosimetric volume in the absence of any shielding material, as shown in the following equation:

$$T(E, d) = D(E, d)/D(E, 0) \quad (2)$$

The transmission rate calculated for 511, 662 and 1332 keV gamma rays as a function of concrete thickness has been shown for ordinary, barite, serpentine and steel-magnetite concretes in Figs. 2–5 respectively.

At first glance, it can be seen from these figures that steel-magnetite concrete with highest density has higher attenuation (lowest transmission) than other concretes. Although barite concrete includes high atomic number elements in compare with other studied concretes, but higher density of steel-magnetite concrete overcomes its higher effective atomic number.

For all three photon energies, it can be deduced that for reduction of gamma ray intensity below a certain rate, ordinary concrete with minimum density (about 2.3 g cm^{-3}) is required in more thickness than other concretes.

Also for these materials and this selection of thicknesses, it is found that the transmission factors (for example in Co-60 gamma rays) for the ordinary, serpentine, barite and steel-magnetite shields span from 1 to less than 10^{-2} , 3×10^{-3} , 10^{-3} and 10^{-5} respectively.

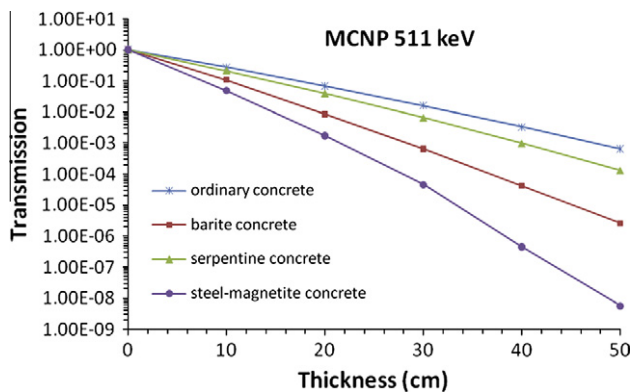


Fig. 2. Transmission factor for four types of concrete in the presence of 511 keV radiation source.

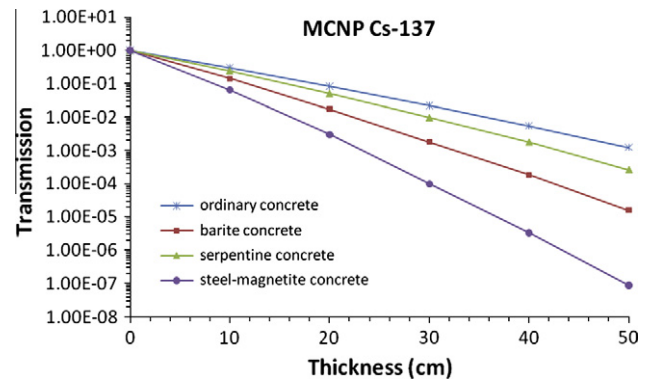


Fig. 3. Transmission factor for four types of concrete in the presence of 662 keV radiation source.

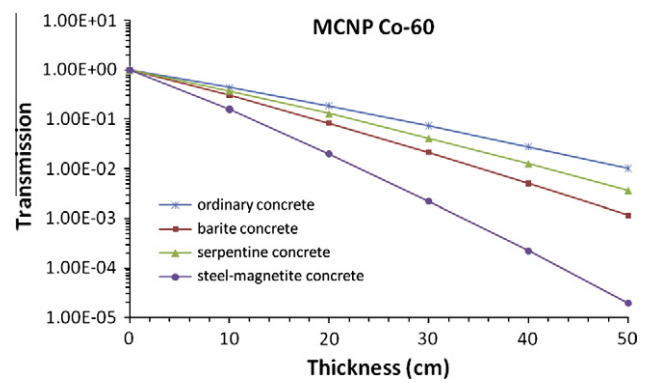


Fig. 4. Transmission factor for four types of concrete in the presence of 1332 keV radiation source.

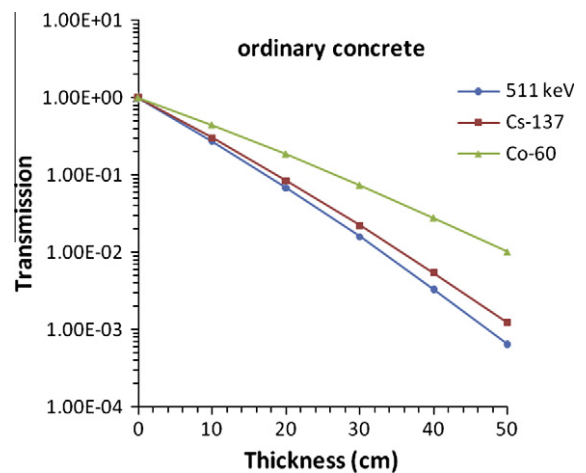


Fig. 5. Transmission factor for 511, 662 and 1332 keV photons versus ordinary concrete thickness.

As can be seen these figures, transmission factors are lower for barite and magnetite loaded concretes than serpentine and ordinary concretes, so barite and magnetite are important and effective materials for using in radiation shielding.

In order to compare the transition rate of 511, 662 and 1332 keV photon energies through identical concrete, transmission factors of these three gamma rays through four types concrete are separately shown in Figs. 5–8.

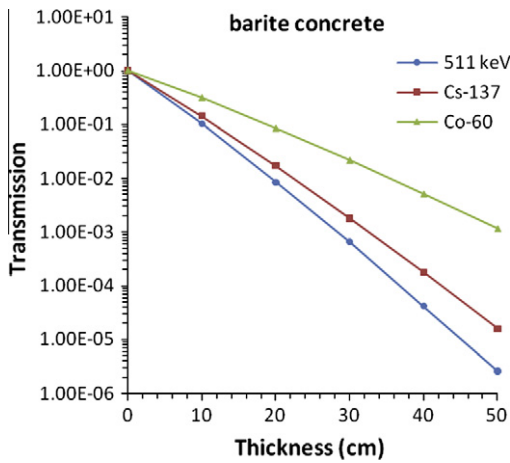


Fig. 6. Transmission factor for 511, 662 and 1332 keV photons versus barite concrete thickness.

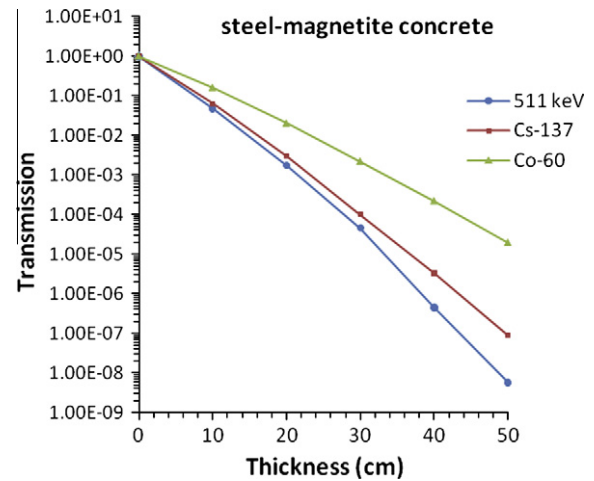


Fig. 8. Transmission factor for 511, 662 and 1332 keV photons versus steel-magnetite concrete thickness.

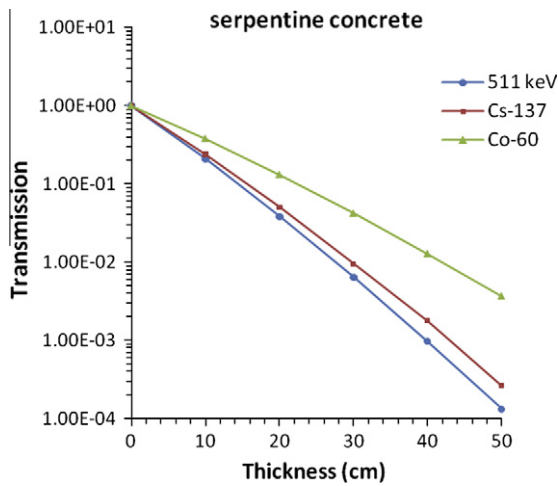


Fig. 7. Transmission factor for 511, 662 and 1332 keV photons versus serpentine concrete thickness.

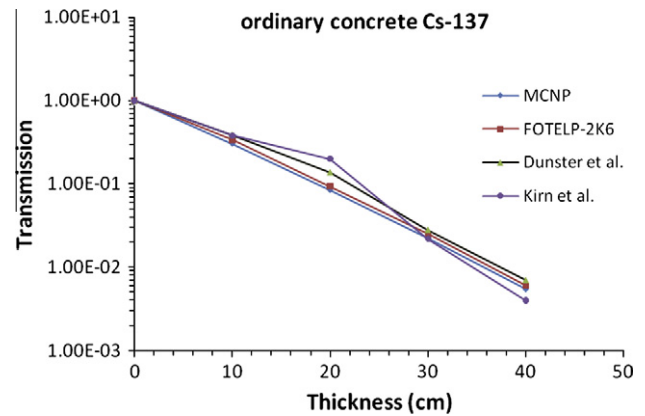


Fig. 9. Transmission factor of 662 keV photon through ordinary concrete (experimental and simulation data).

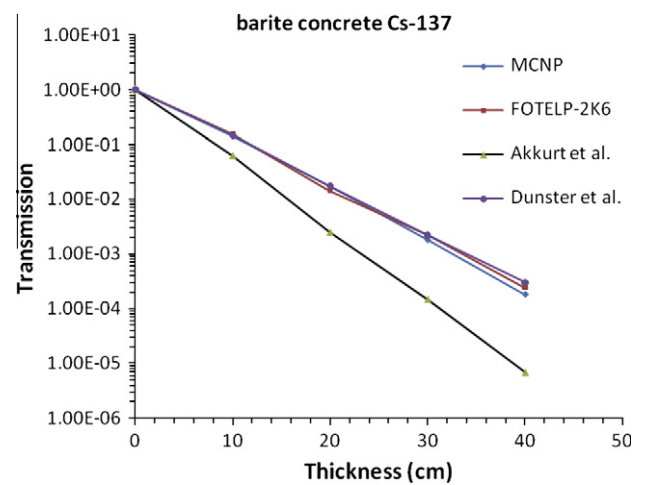


Fig. 10. Transmission factor of 662 keV photon through barite concrete (experimental and simulation data).

It can be clearly seen that in each type of concrete, the higher thickness of concrete is need for higher energy photons because these photons can penetrate through concrete more than photons with lower energies, so their transmission factors are bigger. Annihilation phenomenon Gamma rays carry minimum energy relative to Cs-137 and Co-60 sources and have minimum transmission factors in each type of concrete.

As figures show, differences between transmission factors of these three gamma rays in greater thickness of shields are larger than in smaller thickness of concretes, therefore at smaller thickness of shields regardless of photon energies most of the photons will transmit through concretes.

After simulation by MCNP-4C Code, for comparison and validation of experimental and simulation data, as shown in Figs. 9 and 10, transmission factors of 662 keV photons obtained by MCNP-4C Code in ordinary and barite concrete were compared with several experimental and other simulation data reported in articles.

FOTELP-2K6 code that designed to simulate the transport of photons, electrons and positrons through three-dimensional material and sources geometry by Monte Carlo techniques was employed by Stankovic et al. (2010) and their results along with Kirn et al. (1954); Dunster et al. (1971); Akkurt et al. (2010) experimental data were compared with MCNP calculations.

It is completely clear from both figures that simulation data by MCNP-4C and FOTELP-2K6 codes are very close to each other, because both of them use Monte Carlo techniques for dosimetry and other application of these codes.

Table 3
Linear and mass attenuation coefficients of the concretes.

Concrete type	Ordinary			Barite			Serpentine			Steel–magnetite		
Density (g cm ⁻³)	2.3			3.35			2.6			5.1		
Gamma energy (keV)	511	662	1332	511	662	1332	511	662	1332	511	662	1332
Mass attenuation coefficients (cm ² g ⁻¹)	0.0883	0.0788	0.0560	0.0918	0.0781	0.0520	0.0925	0.0822	0.0585	0.0845	0.0751	0.0528
Linear attenuation coefficients (cm ⁻¹)	0.2031	0.1813	0.1288	0.3076	0.2618	0.1742	0.2406	0.2137	0.1521	0.4312	0.3830	0.2696

Table 4
Experimental and calculational results of linear and mass attenuation coefficients of ordinary and barite concretes.

Concrete type		Ordinary		Barite	
		662	1332	662	1332
Mass attenuation coefficients (cm ² g ⁻¹)	Experiment (I. Akurrt 2010)	0.1044	0.0670	0.0857	0.0490
	Experiment (F. Bouzarjomehri)	–	–	–	0.0540
	Experiment (F. Demir)	0.081	–	–	–
	Calculation	0.0788	0.0560	0.0781	0.0520
Linear attenuation coefficients (cm ⁻¹)	Experiment (I. Akurrt 2010)	0.257	0.165	0.297	0.17
	Experiment (F. Bouzarjomehri)	–	–	–	0.181
	Experiment (F. Demir)	0.187	–	0.261	–
	Calculation	0.1813	0.1288	0.2618	0.1742
Density (g cm ⁻³)	Experiment (I. Akurrt 2010)	2.46	–	3.463	–
	Experiment (F. Bouzarjomehri)	–	–	–	3.35
	Experiment (F. Demir)	2.31	–	–	3.451
	Calculation	2.3	–	–	3.35

Except the Akkurt results Akkurt et al. (2010) in Fig. 10 for barite concrete, experimental data are approximately close to simulation data also reasonable agreement exists between simulated and measured values of both concretes.

Because of the differences in the densities of the ordinary and barite concrete shields used by FOTELP-2K6 and MCNP-4C codes (2.3 g cm⁻³ for ordinary and 3.35 g cm⁻³ for barite concrete), Dunster et al. (1971) (2.36 g cm⁻³ for ordinary), Kirn et al. (1954) (2.35 g cm⁻³ for ordinary) and Akkurt et al. (2010) (3.463 g cm⁻³ for barite concrete) and in the elemental composition of studied concretes in this articles, some inequalities between experimental and simulation data were observed.

Major inequality between experimental results of Akkurt et al. (2010) and other reported data is due to high differences between used barite densities.

As expected, the simulation data similar to experimental data shows that the shielding decreases transmission of gamma rays and totally experimental data are in accordance with simulation results.

3.2. HVL, TVL, linear and mass attenuation coefficients of different concretes

Mass attenuation coefficients of concretes ($\mu_{\text{mass,con}}$) were calculated using Hubbell and Seltzer (2004) data and by Eq. (3) in which, w_i and $\mu_{\text{mass},i}$ are percentage by weight of *i*th element in the concrete and mass attenuation coefficient of *i*th element respectively:

$$\mu_{\text{mass,con}} = \sum_{i=1}^n w_i \times \mu_{\text{mass},i} \quad (3)$$

Also the magnitude of linear attenuation coefficients, μ that can vary with the incident photon energy, the atomic number and the density of the shielding materials were calculated by multiplying mass attenuation coefficient of each type of concrete in its density. Linear and mass attenuation coefficients of each type of concrete obtained by numerical calculations for photon energies interested

in this research were presented in Table 3. For validation of these calculated data, we used experimental results of some concretes available in articles and compared with them in Table 4.

According to these tables, the decrease of mass or linear attenuation coefficients with increasing the photon energy is completely clear for all mentioned concretes. The effect of barite and magnetite along with steel scraps on the linear attenuation coefficient, μ is obvious from both calculation and measured results reported in the articles, thus these two materials are effective in building construction against hazardous gamma radiations. Different densities and fraction of constituent elements of concretes reported by Bouzarjomehri et al. (2006); Akkurt et al. (2010); Demir et al. (2011) and also differences in geometry of modeled configuration relative to experimental geometry lead to little discrepancy in calculation and measured values of linear and mass attenuation coefficients.

The half value layer (HVL) and tenth value layer (TVL) of shielding that are defined as a thickness of concrete specimens that will reduce gamma radiation beam to half and tenth value of its initial intensity respectively, were extracted from transmission diagrams of ordinary and barite concrete and compared with their extrapolated experimental values in Akkurt et al. (2010) work.

The simulated and measured values of HVL and TVL for ordinary concrete in both energies are 1.5–2 times greater than barite concrete. This is derived from high density and high atomic number of barite concrete relative to ordinary concrete. The HVL and TVL de-

Table 5
Measured and simulated results of HVL and TVL for ordinary and barite concretes.

Concrete type		Ordinary		Barite	
		662	1332	662	1332
Gamma energy (keV)		662	1332	662	1332
HVL (cm)	Experiment (I. Akurrt 2010)	2.45	4	2.3	4
	MCNP-4C	5.25	8.23	3.1	6
TVL (cm)	Experiment (I. Akurrt 2010)	8.6	14	7.5	13.8
	MCNP-4C	18	27.3	11.3	18.85
Density (g cm ⁻³)	Experiment (I. Akurrt 2010)	2.46	–	3.463	–
	MCNP-4C	2.3	–	–	3.35

crease with density increasing of the concretes. A difference in the simulated and measured values of HVL and TVL represented in Table 5 is also due to inequalities in densities of concretes.

4. Conclusion

In the present work, transmission factor, linear and mass attenuation coefficients, HVL and TVL values for ordinary, barite, serpentine and steel–magnetite concretes have been calculated and simulated using MCNP-4C Code based on the elemental composition of the concretes, and in order to validation of simulation results, available experimental results reported in references were compared with them.

All simulation results formerly validated by experimental data, demonstrated that steel–magnetite concrete of high density (5.1 g cm^{-3} density) and with constituents of relatively high atomic number relative to other mentioned concretes (with exception of barite concrete) is more effective shield.

Barite concrete with high density and effective atomic number after steel magnetite is a useful concrete as a shield for building construction of nuclear facilities as well. Simulation results for serpentine concrete also indicated that it acts approximately similar to ordinary concrete against gamma rays.

Acknowledgment

The authors are gratefully indebted to Islamic Azad University, Maku Branch for support of this work.

References

- Akkurt, I., Akyıldırım, H., Mavi, B., Kilincarslan, S., Basyigit, C., 2010. Photon attenuation coefficients of concrete includes barite in different rate. *Ann. Nucl. Energy* 37, 910–914.
- Bashter, I.I., 1997. Calculation of radiation attenuation coefficients for shielding concretes. *Ann. Nucl. Energy* 24 (17), 1389–1401.
- Bouzarjomehri, F., Bayat, T., Dashti, R.M.H., Ghisari, J., Abdoli, N., 2006. ^{60}Co γ -ray attenuation coefficient of barite concrete. *Iran J. Radiat. Res.* 4, 71–75.
- Brice, David, K., 1984. Stopping powers for electrons and positrons. Report 37, ICRU. *Nucl. Instr. Meth. B* 12, 187–188.
- Cember, H., Johnson, E., 2009. *Introduction to Health Physics*, fourth ed. Department of Environmental and Radiological Health Sciences Colorado State University, Fort Collins, Colorado.
- Demir, F., Budak, G., Sahin, R., Karabulut, A., Oltulu, M., Un, A., 2011. Determination of radiation attenuation coefficients of heavyweight- and normal-weight concretes containing colemanite and barite for 0.663 MeV γ -rays. *Ann. Nucl. Energy* 38, 1274–1278.
- Dunster, H.J., Ellis, R.E., Jones, B.E., Jones, E.W., Rees, J.M., 1971. *Handbook of Radiological Protection. Part 1. Data.* Radioactive Substances Advisory Committee HMSO, London.
- Eakins, J., 2007. An MCNP-4C2 determination of gamma source shielding health protection agency center for radiation, chemical and environmental hazards radiation protection division ISBN 978-0-85951-603-7.
- Hubbell, J.H., Seltzer, S.M., 2004. *Tables of X-ray Mass Attenuation Coefficients and Mass Energy-Absorption Coefficients (Version 1.4).* National Institute of Standards and Technology, Gaithersburg, Md., USA.
- Kirn, F.S., Kennedy, R.J., Wyckoff, H.O., 1954. *Radiology* 63, 94.
- Shultis, J.K., Faw, R.E., 2010. *An MCNP PRIMER* Department of Mechanical and Nuclear Engineering. Kansas State University.
- Stankovic, S.J., Ilic, R.D., Jankovic, K., Bojovic, D., Longar, B., 2010. Gamma radiation absorption characteristics of concrete with components of different type materials. *Acta Phys. Pol. A* 117, 812–816.